Diaphorocetus poucheti (Cetacea, Odontoceti, Physeteroidea) from Patagonia, Argentina: one of the earliest sperm whales

Florencia Paolucci, Mónica R. Buono, Marta S. Fernández, Felix G. Marx & José I. Cuitiño

View supplementary material

Published online: 14 Jun 2019.

Submit your article to this journal

View Crossmark data

Taylor & Francis
Taylor & Francis Group

Check for updates

Diaphorocetus poucheti (Cetacea, Odontoceti, Physeteroidea) from Patagonia, Argentina: one of the earliest sperm whales

Florencia Paolucci[a] , Mónica R. Buono[b], Marta S. Fernández[c]* , Felix G. Marx[c,d,e,f] and José I. Cuitiño[b]

[a]*CONICET – División Paleontología Vertebrados, Unidades de Investigación, Anexo Museo, Facultad de Ciencias Naturales y Museo, Universidad Nacional de La Plata, 60 y 122, 1900 La Plata, Argentina;* [b]*Instituto Patagónico de Geología y Paleontología, CENPAT-CONICET, Bvd. Brown 2915, U9120ACD, 9120, Puerto Madryn, Chubut, Argentina;* [c]*Department of Geology, University of Liège, B18, Quartier Agora, 14 Allée du 6 Août, 4000 Liège, Belgium;* [d]*Directorate of Earth and History of Life, Royal Belgian Institute of Natural Sciences, Vautierstreet, 29, 1000 Brussels, Belgium;* [e]*School of Biological Sciences, Monash University, Wellington Rd, Clayton VIC 3800, Australia;* [f]*Geosciences, Museum Victoria, 11 Nicholson St, Carlton VIC 3053, Australia*

Sperm whales (Physeteroidea) are the basal-most surviving lineage of odontocetes, represented today by just three highly specialized, deep-diving suction feeders. By contrast, extinct sperm whales were relatively diverse, reflecting a major Miocene diversification into various suction feeding and macroraptorial forms. The beginnings of this diversification, however, remain poorly understood. The Atlantic coast of South America provides a crucial window into early physeteroid evolution and has yielded some of the oldest species known from cranial material, *Idiorophus patagonicus* and *Diaphorocetus poucheti* – both of which are in need of re-description and phylogenetic reappraisal. Here, we re-examine *Diaphorocetus* in detail and, in light of its complex taxonomic history, declare it a *nomen protectum*. Phylogenetically, the species forms part of a polytomy including '*Aulophyseter*' *rionegresis* and the two crown lineages (Physeteridae and Kogiidae) and demonstrates that facial asymmetry and a clearly defined supracranial basin have characterized this lineage for at least 20 Ma. With a total body length of 3.5–4 m, *Diaphorocetus* is one of the smallest physeteroids yet known. Its cranial morphology hints at an intermediate raptorial/suction feeding strategy and it has a moderately developed spermaceti organ and junk.

Keywords: Physeteroidea; Gaiman Formation; phylogeny; anatomy; body size; Miocene

Introduction

Sperm whales are among the most bizarre of all cetaceans, thanks to their highly modified cranial morphology and oversized narial complex. They are characterized by strongly asymmetrical external bony nares (with the left being markedly larger) and the presence of a pronounced dorsal concavity – the supracranial basin – housing the spermaceti organ (e.g. Flower 1868; Cranford *et al.* 1996).

Extant sperm whales are represented by just three species: the giant sperm whale (*Physeter macrocephalus* Linnaeus, 1758), and the pygmy and dwarf sperm whales (*Kogia breviceps* de Blainville, 1838 and *K. sima* Owen, 1866, respectively). By contrast, extinct physeteroids were far more diverse and comprised a disparate assemblage of suction feeders and macroraptorial predators (e.g. Cozzuol 1993, 1996; Bianucci & Landini 2006; Kimura & Hasegawa 2006; Lambert *et al.* 2008, 2010, 2016; Boersma & Pyenson 2015; Velez Juarbe *et al.* 2015). Molecular divergence dating

places the origin of sperm whales in the late Oligocene (McGowen *et al.* 2009), coincident with their oldest known stratigraphical occurrence (Mchedlidze 1970).

At present, physeteroid diversity seems to be concentrated primarily in the middle–late Miocene. This pattern is plausible but complicated by the general scarcity of early Miocene fossils, inflated diversity estimates driven by waste-bin taxa (e.g. *Scaldicetus*; see Bianucci & Landini 2006), and phylogenetic disagreements. Thus, while the monophyly of kogiids is generally agreed upon (e.g. Bianucci & Landini 1999, 2006; Lambert 2008; Lambert *et al.* 2010, 2016; Velez Juarbe *et al.* 2015), the relationships of physeterids and stem physeteroids remain contentious. For example, macroraptorial species are often grouped together on ecomorphological grounds (e.g. Bianucci & Landini 2006; Lambert *et al.* 2016) yet have never been formally recovered as a clade.

Eastern Patagonia is one of relatively few localities that have produced a rich early Miocene cetacean

---

*Corresponding author. Email: martafer@fcnym.unlp.edu.ar

assemblage (Buono *et al.* 2017; Viglino *et al.* 2018a, b), and thus holds particular promise for elucidating the early evolutionary history of sperm whales. In particular, widespread outcrops of the Gaiman Formation in Chubut Province (Argentina) have yielded the two oldest physeteroids known from cranial material: *Idiorophus patagonicus* (Lydekker, 1893 [1894]) and *Diaphorocetus poucheti* (Moreno, 1892).

Diaphorocetus poucheti was originally described by Moreno (1892) and subsequently revised by Lydekker (1893) [1894] and Ameghino (1894a). Despite its significance, it has not been re-studied in detail since, even though it has featured in several phylogenetic analyses. The latter recovered *D. poucheti* as either a stem physeteroid (Bianucci & Landini 2006; Lambert 2008; Lambert *et al.* 2008), or as deeply nested within Physeteridae (Lambert *et al.* 2016), revealing considerable phylogenetic uncertainty. Here, we provide a detailed re-description of this crucial species, clarify several morphological details, and present an updated phylogenetic analysis of Physeteroidea.

Taxonomic background

Moreno (1892) illustrated and briefly described *Mesocetus poucheti* based on an incomplete skull without teeth (MLP 5-6; Moreno 1892, pl. X; fig. 1A), noting that the new taxon shared some features with sperm whales. Subsequently, Moreno, in his capacity as the director of the Museo de La Plata, invited Richard Lydekker to study the resident collection of vertebrate fossils. Lydekker published his findings in the *Anales del Museo de La Plata*, under the title "Contributions to knowledge of the fossil vertebrates of Argentina: (II). Cetacean skulls from Patagonia". The date of publication, as printed on the cover page, was 1893, and the prologue was signed by Lydekker in November of that year (Supplementary material 1, Appendix 1). The accuracy of this date has been questioned, however, with some authors considering the paper to have appeared in 1894. This has created much taxonomic confusion, as detailed below.

On p. 7, Lydekker (1893) [1894] noted that the name *Mesocetus* was preoccupied by a genus created by Van Beneden (1880) for an extinct mysticete from Belgium, and proposed *Hypocetus* as a substitute. On the next page, Lydekker introduced yet another name, *Paracetus*, for the same material, making *Hypocetus* and *Paracetus* objective synonyms. In a subsequent paper, Lydekker (1894, p. 125) reverted to *Hypocetus*. Cope (1895, p. 135), however, failed to notice Lydekker's (1893) mistake, and used *Paracetus* to refer the species to Physeteridae for the first time. Independently, Ameghino (1894a, p. 181), unaware of Lydekker's

(1893) paper, also recognized the homonymy of *Mesocetus* Moreno, 1892, and proposed *Diaphorocetus* to replace it.

Kellogg (1925, p. 3) summarized the taxonomic status of Patagonian physeteroids, which by then had received four different names (*Mesocetus*, *Paracetus*, *Hypocetus* and *Diaphorocetus*) and cited Lydekker's contribution as "Anales del Museo de La Plata, vol. 2, for 1893, p. 8. April, 1894". Believing that Ameghino's article was published two months before Lydekker's, he proposed *Diaphorocetus* Ameghino, 1894a as the correct name. This opinion was followed by Cabrera (1926) and all subsequent studies.

After an intense bibliographic search at the library and the Archivo Histórico of the Museo de La Plata, we could not find any evidence that Lydekker's contribution was published in 1894, as had been claimed by Ameghino (1894b), Kellogg (1925) and Cabrera (1926). We thus consider the date printed on the cover page and prologue – 1893 – to be the actual date of publication. Nevertheless, *Hypocetus* and *Paracetus* have not been used since 1899 and therefore – although available – should be considered *nomina oblita* under Articles 23.9.1.1 and 23.9.2 International Code of Zoological Nomenclature (ICZN). *Diaphorocetus*, by contrast, has been used in more than 25 publications by more than 10 authors (see Systematic palaeontology, below) from 1894 to 2016, thereby satisfying the requirements for a *nomen protectum* under Articles 23.9.1.2 and 23.9.2 (ICZN).
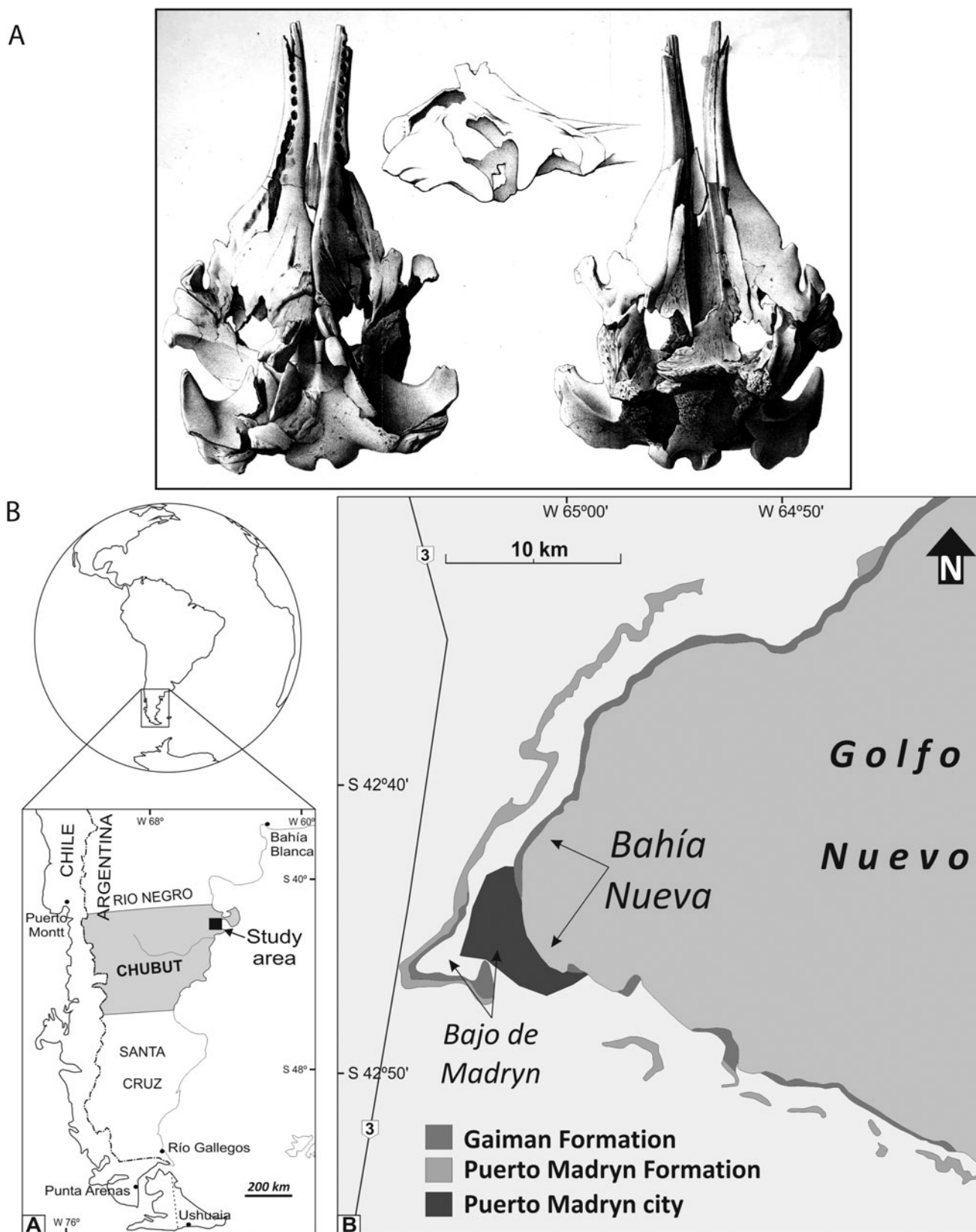
Institutional abbreviations

IRSNB: Institut royal des Sciences naturelles de Belgique, Brussels, Belgium; **MACN**: Museo Argentino de Ciencias Naturales, Buenos Aires, Argentina; **MLP**: Museo de La Plata, La Plata, Argentina; **MNHN**: Museum national d'Histoire naturelle, Paris, France; **USNM**: National Museum of Natural History, Smithsonian Institution, Washington, DC, USA.

Material and methods

Specimens analysed

The anatomical description of *Diaphorocetus poucheti* is based on the holotype and only known specimen (MLP 5-6). Material used for comparison includes personal observations by FP, as follows: *Physeter macrocephalus* (MACN-Ma 29768, MACN-Ma 20518, USNM 35315); 'Aulophyseter' *rionegrensis* (MLP 62-XII-19-1); *Preaulophyseter gualichensis* (MLP 76-IX-5-1); *Physeterula dubusi* (IRSNB M.527/3192); *Eudelphis mortezelensis* (IRSNB M.523); *Placoziphius duboisi* (IRSNB M.530/1718); *Orycterocetus crocodilinus*

Figure 1. A, original drawing of the holotype cranium of *Diaphorocetus poucheti* by G. Bauer (lithographic artist of the Museo de La Plata) in ventral (left), lateral (centre) and dorsal view (right). **B,** maps of the study area, indicating the extent of the Gaiman and Puerto Madryn formations and the location of the city of Puerto Madryn.

(IRSNB M.1936); *Thalassocetus antwerpiensis* (IRSNB M.525); *Scaphokogia cochlearis* (MNHN PPI229, MNHN PPI240); *Acrophyseter deinodon* (MNHN SAS 1626). It also includes information from photographs or the literature: *Zygophyseter varolai* (MAUL 229/1); *Idiorophus patagonicus* (MLP 5-2); *Aulophyseter morricei* (USNM 11230); *Orycterocetus crocodilinus* (USNM 22926); *Physeter macrocephalus* (USNM 49488); *Livyatan melvillei* (USNM 1676).

Methods

Anatomical terminology follows Mead & Fordyce (2009). Most of the measurements follow Perrin (1975). To determine physical maturity, we assessed the closure of the cranial sutures following Perrin (1975) and Galatius (2009), who based their criteria on *Cephalorhynchus*, *Lagenorhynchus* and *Stenella*. Total body length (TL) was calculated based on bizygomatic width (BZW) and condylobasal length (CBL), using the equations of Pyenson & Sponberg (2011) – $\log_{10}(TL) = 0.92 \times (\log BZW - 1.68) + 2.64$ – and Lambert *et al.* (2010) – $TL = 4.23 \times BZW + 222.04 + CBL$. Photographs were taken with a Nikon D7200 camera and an 18–140 mm Nikkor vr2 lens.

Phylogenetic analysis

We adapted the morphological matrix of Lambert *et al.* (2016). Prior to analysis we merged their characters (char.) 13 and 20 (now char. 14, widening of the right premaxilla), and added two characters (char. 6, mesorostral groove; char. 30, long axis of skull) from Boersma & Pyenson (2015) and Velez-Juarbe *et al.* (2015), respectively. We furthermore amended the previous scorings for *Diaphorocetus*, which were based largely on the literature, with our own direct observations. The orbital region of the holotype cranium is damaged, but could be scored (chars 24, 26 and 43) based on photos taken during the 1980s by C. de Muizon.

The final matrix included 27 taxa and 54 characters (Supplementary material 1, Appendix 2) and was analysed via a traditional search (2000 replicates, with random addition sequences followed by Tree Bisection and Re-connection (TBR) branch-swapping, holding 10 trees per replicate) and implied weighting (k = 3, 10, 20) in TNT v. 1.5 (Goloboff *et al.* 2008a, b). The resulting most parsimonious trees (MPTs) were summarized in a strict consensus with zero-length branches collapsed ('rule 1' of Coddington & Scharff 1994). Branch support was assessed using Bremer decay values. To identify unstable taxa we use the IterPCR procedure (Pol & Escapa 2009; Escapa & Pol 2011) over the entire set of MPTs (Supplementary material 1, Appendix 3). Finally, we scaled our strict consensus tree according to the stratigraphical ranges of all including

species (Supplementary material 1, Appendix 4), using the timePaleoPhy function of the Paleotree package in R (version 3.4.4). The TNT file used in our analyses is supplied as Supplementary material 2.

Systematic palaeontology

Cetacea Brisson, 1762
Neoceti Fordyce & de Muizon, 2001
Odontoceti Flower, 1867
Physeteroidea Gray, 1821
Diaphorocetus Ameghino, 1894a *nomen protectum*

Type species. *Diaphorocetus poucheti.*

Diagnosis. As for the type and only species.

Diaphorocetus poucheti (Moreno, 1892)
(Figs 2–8)

1892 *Mesocetus poucheti* Moreno: 395–397, pl. X (*non* Van Beneden, 1880).
1893 *Hypocetus poucheti* (Moreno) Lyddeker: 7, pl. III *nomen oblitum*.
1893 *Paracetus poucheti* (Moreno) Lyddeker: 8; Cope 1895: 135 *nomen oblitum*.
1894 *Diaphorocetus poucheti* (Moreno) Ameghino: 1894a; Allen 1921: 155; Ameghino 1921: 2; Kellogg 1925: 2–17; 1928: 34, 176–178; 1965: 49; Cabrera 1926: 408–409; de Muizon 1991: 298; Raven & Gregory 1933: 6, 14; Cozzuol 1993: 21, 33; 1996: 324; Hirota & Barnes 1994: 453–455, 468; Heyning 1997: 599; Bianucci & Landini 1999: 450–451; 2006: 105, 120, 123, 125–126, 130–131; Kázar 2002; 151–152, 158–163; Fordyce 2009: 212; Hampe 2006: 61, 62, 64, 65, 76, 80, 82; Canto 2007: 10; Lambert 2008: 279, 282, 284, 287, 288, 291, 292, 300, 302, 306–309, 315; Lambert *et al.* 2008: 362, 366, 369; 2016: 4, 10, 11, 13, 14, 47, 58, 60, 61; Mchedlidze 2009: 1097–1098; Pérez *et al.* 2011: 648–649; Cione *et al.* 2011: 428; Toscano *et al.* 2013: 440; Buono 2014: 33; Boersma & Pyenson 2015: 7, 26; Collareta *et al.* 2017: 273.

Material. MLP 5-6 (holotype), fragmentary skull lacking the teeth, mandibles and tympanoperiotic bones.

Type locality and age. According to Moreno (1892, p. 395), the holotype was recovered from "tertiary strata from Bahía Nueva, Chubut, at *42°30′S* latitude, likely Miocene". No additional information is available at the MLP. Bahía Nueva is a small bay located to the west of Golfo Nuevo (north-western Chubut Province, Argentina), and is today the location of the city of

Puerto Madryn ([Fig. 1B](#)). Two Miocene marine deposits are exposed in this area: the early Miocene Gaiman Formation (Burdigalian *c.* 20–18 Ma) and the late Miocene Puerto Madryn Formation (Haller *et al.* 2005; Cuitiño *et al.* 2017). Both units are sub-horizontal, with the Gaiman Formation being exposed along the coastal cliffs and low hills, and the overlying Puerto Madryn Formation occupying higher topographic positions farther inland ([Fig. 1B](#); Haller *et al.* 2005). The fact that Moreno (1892) mentioned Bahia Nueva, rather than 'Bajo de Madryn' (a lowland to the west of the gulf; [Fig. 1B](#)), suggests that the holotype of *D. poucheti* came from the coastal zone, i.e. the wave-cut platform or coastal cliffs, both of which expose the Gaiman Formation ([Fig. 1B](#)). This interpretation is further supported by whitish mudstone still attached to the specimen, which is consistent with the lithology of the Gaiman Formation in this area. If this interpretation is correct, then *Diaphorocetus* most likely dates to the late early Miocene (Burdigalian), *c.* 20–18 Ma (see review in Cuitiño *et al.* 2017).

Emended diagnosis. Small-sized physeteroid (3.5–4 m long) characterized by the following unique combination of characters: dorsoventrally flattened skull with an oblique occipital shield, rostrum shaped like a bottleneck and contributing 50% of CBL, at least 10 deep maxillary alveoli separated by wide interalveolar septa, supracranial basin low and not extending onto the rostrum or right orbit, and temporal fossa wide and short. Differs from other physeteroids in having a zygomatic process of the squamosal with a ventrally deflected (rather than horizontal) apex; from physeterids in having a ventrally oriented postorbital process of the frontal; from '*Aulophyseter*' *rionegrensis* in having a smaller skull (11%, based on BZW), wide and well-developed upper interalveolar septa, an obliquely oriented occipital shield, a dorsoventrally flattened skull, a shorter temporal fossa and a narrower exposure of the parietal in the temporal fossa; from *Idiorophus* in having a smaller skull, an open mesorostral groove, a flatter cranium and smaller dorsal infraorbital foramina; from *Aulophyseter morricei* in having a narrower tip of the rostrum, an open mesorostral groove, a longer zygomatic process (ratio between length of zygomatic process and CBL = 0.29), a longer temporal fossa and less posteriorly protruding occipital condyles; from *Placoziphius* in having deep alveoli, a larger palatal exposure of the vomer, and a more open jugular notch; from *Eudelphis* in having thick and well developed upper interalveolar septa, a rostrum shaped like a bottleneck and a dorsoventrally shorter postglenoid process; from *Physeterula* in having a smaller (by *c.* 30%) and more flattened cranium, and a convex occipital shield (in lateral view); from *Orycterocetus crocodilinus* in having a convex occipital

shield, a lower supracranial basin, deep upper alveoli and wider upper interalveolar septa; from *Idiophyseter* in having less posteriorly protruding occipital condyles, a more laterally situated right premaxillary foramen and a flattened skull; from *Physeter* in having a smaller skull (by *c.* 70%) whose long axis is roughly horizontal, a supracranial basin that does not extend onto the rostrum, deep upper alveoli, a convex occipital shield, a lower supracranial basin and a rostrum that is shaped like a bottleneck; from Kogiidae in having a longer rostrum, and in lacking a sagittal crest; and from *Livyatan*, *Zygophyseter* and *Acrophyseter* in having a smaller temporal fossa, smaller teeth (greatest transverse diameter of root < 5% of BZW) and a flattened skull.

Description

Preservation
The cranium is eroded and lacks the ear bones, mandibles, teeth and a portion of the vertex. The rostrum is broken along the sagittal plane, deformed on its left side and detached from the remainder of the cranium, with no clean breakage surfaces that might allow re-articulation. Owing to taphonomic deformation and the fact that the original reconstruction of the fossil was carried out over a century ago, it is likely that some bones are not in their correct anatomical position. The state of the specimen has notably degraded since its original description and the orbital regions are now missing. As a result, we are forced to base some of our observations on the illustrations provided by Moreno (1892, pl. X) and photos taken by C. de Muizon in the 1980s.

Physical maturity
The cranial sutures are closed but visible, suggesting an ontogenetic state equivalent to Class IV or V of Perrin (1975). The external surface of the occipital condyles is smooth rather than pitted, as in juveniles. Together, these observations suggest a subadult individual.

Body length
We estimate a total body length of 3.46 m following Pyenson & Sponberg (2011) or 3.25 m following Lambert *et al.* (2010). The difference between these two estimates may arise from the incomplete rostrum, which forced us to estimate condylobasal length.

General description
The maxilla and premaxilla extend posteriorly towards the occipital region and there form a distinct

Table 1. Measurements (mm) from the skull of *Diaphorocetus poucheti* (MLP 5-6, holotype).

Measurement	mm
Bizygomatic width of skull	522.9
Condylobasal length	820*
Rostrum length	491.9*
Cranium length	325.8*
Length of preserved right premaxilla on rostrum	222.4
Width of rostrum at level of antorbital notches	388*
Width at preserved tip of rostrum	83.6*
Length of antorbital notch	40.5
Distance between lateral margins of rostrum and anterior-most preserved alveolus	8.7
Distance between lateral margins of rostrum and posterior-most preserved alveolus	14.7
Height of temporal fossa	131.3
Length of temporal fossa	93.4
Transverse depth of temporal fossa	164.7
Length of zygomatic process	154.4
Maximum width of ventral exposure of vomer on rostrum	44.1
Minimum distance between temporal fossae across supraoccipital shield	225.3
Width of supracranial basin	278.8
Height of occipital condyle	74.4
Width of occipital condyle	41.8
Maximum distance between lateral margins of occipital condyles	137.2
Height of foramen magnum	56.6
Transverse diameter of foramen magnum	54.2
Distance between antorbital notch and right premaxillary foramen	248,4
Length of alveoli	15.2
Width of alveoli	10.3
Maximum width of premaxilla on rostrum	52.2
Width of lateral exposure of parietal in temporal fossa	31.3
Preserved height of lateral exposure of parietal in temporal fossa	81.9*
Anterior extension of palatine with respect to antorbital notch	70.3
Width of ventral exposure of alisphenoid	99.5
Length of ventral exposure of alisphenoid	104.7
Length of basioccipital crest	93.6
Width of basioccipital crest	56.4
Width of basilar part of basioccipital	174.6
Width of intercondylar notch	32.6
Length of right premaxillary foramen	21.4*
Width of right premaxillary foramen	16.4
Distance between anterior tip of zygomatic process and ventral tip of postglenoid process	147.8
Length of alveolar line	287.2*

*Incomplete.

supracranial basin. The skull is flattened dorsoventrally and has an overall pentagonal outline in dorsal view. Its CBL of *c.* 820 mm matches that of several small- to medium-sized physeteroids (e.g. *Orycterocetus crocodilinus*, *Eudelphis*, *Idiophyseter*, *Placoziphius*, *Acrophyseter deinodon*), but is notably shorter than in other Patagonian sperm whales ('*Aulophyseter*' *rionegrensis* = 1035 mm, *Idiorophus* = 1140+ mm, based on the mandibles).

The rostrum contributes about half of the total length of the skull and is shaped like a bottleneck in dorsal view, with a narrow tip ($\sim$ 84 mm), a wider posterior portion ($\sim$388 mm just anterior to the antorbital notch) and a concave lateral border. This shape also occurs in *Placoziphius*, *Orycterocetus crocodilinus*, *Aulophyseter morricei* and '*Aulophyseter*' *rionegrensis*, but contrasts with the more triangular rostrum of other physeteroids (e.g. *Physeter*, *Livyatan* and *Zygophyseter*). There are eight well-preserved alveoli in each maxilla and at least two or three others in a more fragmentary condition. Like the rostrum as a whole, the maxilla distinctly widens posterolaterally. The dorsal surfaces of both the rostrum and the supracranial basin are largely lost. The temporal fossa is oval in lateral view and large relative to BZW. The ratio between the minimum distance between the temporal fossae and the BZW is 0.43, similar to that of *Acrophyseter robustus* (0.44).

Premaxilla. In dorsal view, the premaxilla is narrow at the tip, but then widens posterolaterally (Table 1). There is no anterior constriction as seen in *Livyatan*. The right premaxillary foramen is fragmentary and positioned
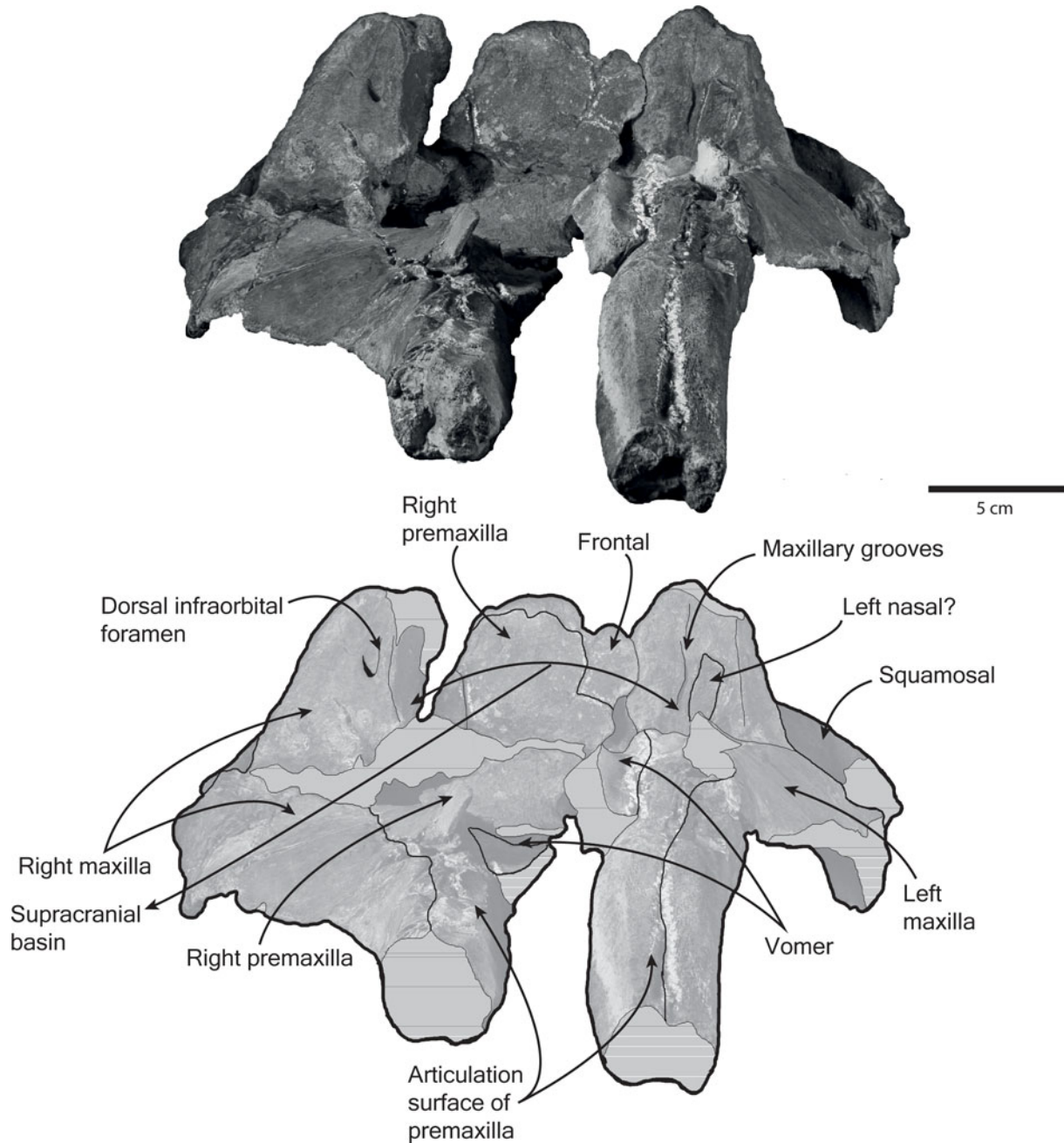
Figure 2. Holotype cranium of *Diaphorocetus poucheti* (MLP 5-6) in anterior view. **A,** photograph; **B,** explanatory line drawing. Hatched areas indicate broken and eroded surfaces; dark shading indicates natural cavities.

medial to the antorbital notch. The position of the left premaxillary foramen may be indicated by grooves and a canal located 145 mm anterior to the level of the antorbital notch, at the suture with the maxilla. The right premaxilla extends farther posteriorly than the left, gradually widens, crosses the sagittal plane and contributes to the supracranial basin, probably without overhanging the right orbit (Fig. 2). Inside the supracranial basin, the premaxillae are notably eroded, obscuring most

morphological detail. Nevertheless, there is no evidence that the supracranial basin extended onto the rostrum. The right external bony naris is partially preserved and notably displaced to the left, suggesting strong facial asymmetry (Fig. 3).

In lateral view, the rostral portion of the premaxilla contacts the maxilla along a straight, approximately horizontal, suture and forms a dorsally convex blade that overhangs the mesorostral groove. Several foramina
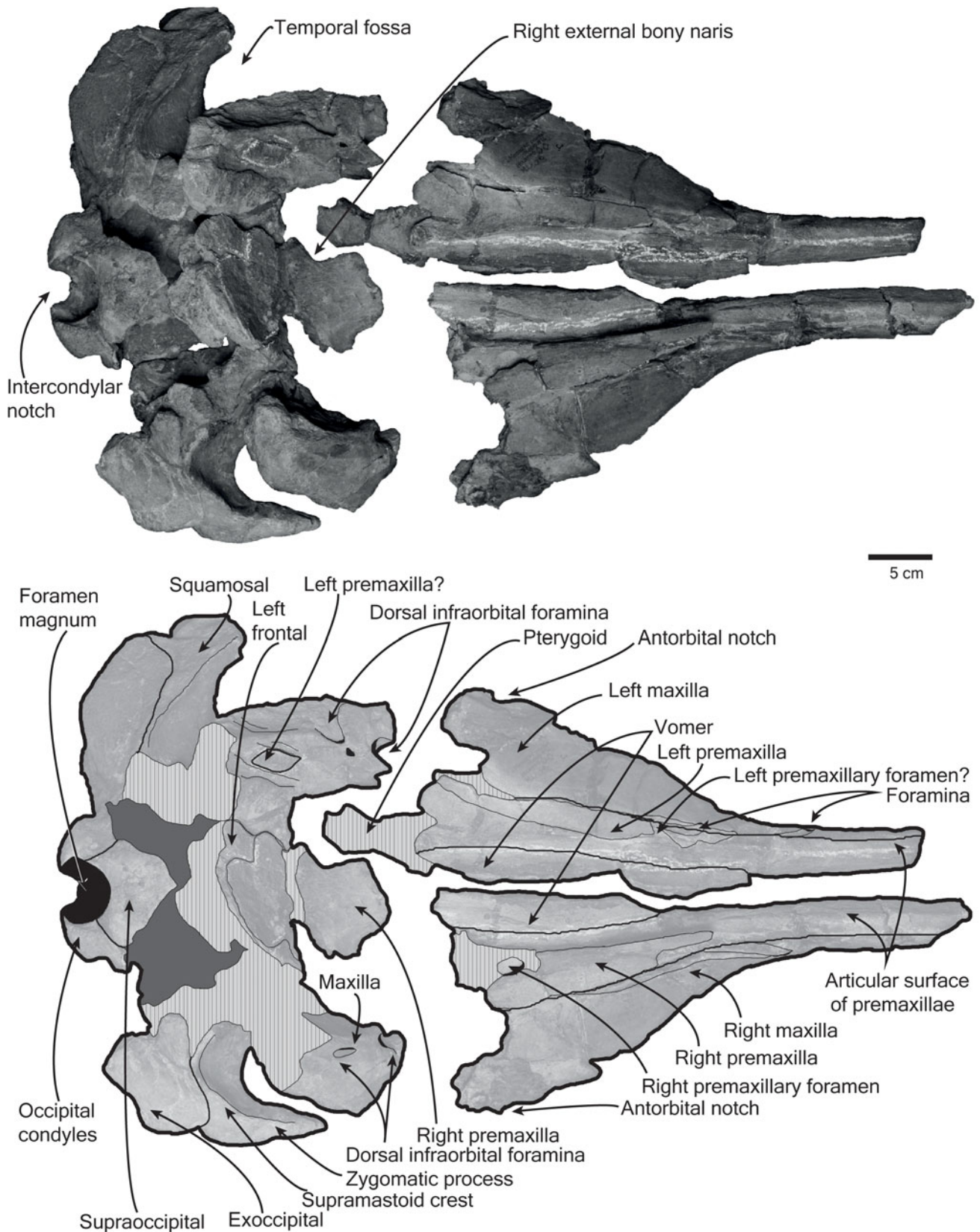
Figure 3. Holotype cranium of *Diaphorocetus poucheti* (MLP 5-6) in dorsal view. **A,** photograph; **B,** explanatory line drawing. Light shading indicates missing parts; hatched areas indicate broken and eroded surfaces; dark shading indicates natural cavities.

along the articular surface of the left premaxilla (i.e. on the left maxilla; Fig. 3) may indicate the presence of well-developed premaxillary sacs (Lambert 2008). These foramina are absent in extant physeteroids, but present in all other odontocetes, and thus may represent a plesiomorphic feature. In ventral view, the premaxilla is exposed on the palate between the tip of the rostrum and the tip of the vomer.

Maxilla. The rostral portion of the left maxilla is broken and turned outwards. In dorsal view, the maxillae widen posterolaterally and contribute to the antorbital notches, which were figured as deep, narrow and asymmetrical by Moreno (1892, pl. X; fig. 1). Both maxillae furthermore contribute to the lateral boundaries of the poorly preserved supracranial basin, which is flanked on either side by at least two unevenly sized dorsal infraorbital foramina (the more anterior one being the larger). The position of these foramina is asymmetrical, with the pair on the right being located more posteriorly (Fig. 3). Grooves on the maxilla along the left margin of the supracranial basin likely correspond to additional foramina, and together delimit a flat bone that may be part of the left premaxilla. The antorbital processes have broken away from the bulk of the cranium but remain attached to the lacrimals along a visible suture (Fig. 4).

In ventral view, the maxilla is consistently wider than the premaxilla and forms most of the palate. There are at least 10 alveoli in each maxilla, including eight with well-defined margins on the left and five on the right. The alveoli are deep, similar in size and oblique, implying anteriorly oriented upper teeth (Fig. 5). Posteriorly, the tooth row terminates *c.* 200 mm anterior to the antorbital notch. The interalveolar septa are thick and well defined, with the anterior alveoli being more closely spaced (*c.* 7 mm) than the posterior ones (*c.* 11 mm). Two shallow depressions located medial to the tenth alveolus may represent embrasure pits for the lower teeth (Supplementary material 1, Appendix 6).

Vomer. In dorsal view, the lanceolate vomer floors the mesorostral canal along the posterior portion of the rostrum. On the right, the suture between the premaxilla and the vomer curves outwards, in tandem with the widening of the right premaxilla; posteriorly, the suture cannot be traced (Fig. 3). The mesorostral groove is damaged, but appears to have been wide, deep and open dorsally. In ventral view, the preserved portion of the vomer is exposed on the palate and contacts the premaxilla along a curved suture, the maxilla along a parasagittal suture and the palatine along an anteriorly convex suture.

Lacrimojugal. Small portions of both lacrimojugals are preserved and form the ventral portion of the antorbital processes. In dorsal view, the right antorbital process of the maxilla has two lateral protuberances connected by a low crest: one at the anterolateral corner, the other about 4 cm posteromedial to the first in a straight line (Fig. 4A). The lacrimojugal/maxilla suture is sigmoidal in anterolateral view (Fig. 4B, C) and approximately horizontal, with the maxilla extending laterally beyond the jugal. The left lacrimojugal is deformed (Fig. 4D–F).

Frontal and parietal. Only a small portion of the frontal remains, with the originally preserved orbital margin now missing. In lateral view, the coronal suture is subvertical and relatively straight. By contrast the, fronto-maxilla suture forms an angle of about 25° with the horizontal plane of the skull. Based on de Muizon's photographs (Supplementary material 1, Appendix 5), the postorbital process is thick, triangular, oriented ventrally and about as long (65 mm) as the diameter of the orbit. The orbital rim of the frontal appears robust, with a rounded preorbital process that is roughly aligned with the lateral margin of the rostrum. In ventral view, the optic canal forms an angle of *c.* 50° with the sagittal plane (Fig. 5). The exposure of the parietal in the temporal fossa is approximately rectangular, and posteriorly delimited by a vertical suture with the squamosal. There is no contact of the parietal with the alisphenoid.

Palatine and pterygoid. In ventral view, the palatine forms a wide (82 mm), anteriorly blunt triangle (Fig. 5), and extends 70 mm anterior to the level of the antorbital notch. There are no obvious palatine foramina. The palatine/maxilla suture is straight and oriented obliquely with respect to the sagittal plane. The pterygoid is narrow anteriorly and overlaps the palatine along a roughly rectangular suture (Fig. 6A, B). Anteromedially, the pterygoids are separated from each other by a posterior extension of the palatines. The posterior lamina is externally excavated by the pterygoid sinus and relatively elongate, as in *Acrophyseter deinodon* (Lambert *et al.* 2016); its suture with the basioccipital is more evident on the right (Fig. 6C, D). The hamular process has a rounded posterior margin and extends posteriorly approximately to the level of the tip of the zygomatic process.

Exoccipital. Both exoccipitals are preserved, but highly eroded. In posterior view, the exoccipital is wide (Fig. 7A), robust laterally and contributes to the posterodorsally facing occipital shield. The occipital condyles are robust and covered by smooth articular facets. The intercondylar notch is wide (33 mm) and 'U'-shaped and the foramen magnum is approximately circular. The jugular notch is wide and 'U'-shaped and oriented ventrolaterally. The paroccipital process is small,
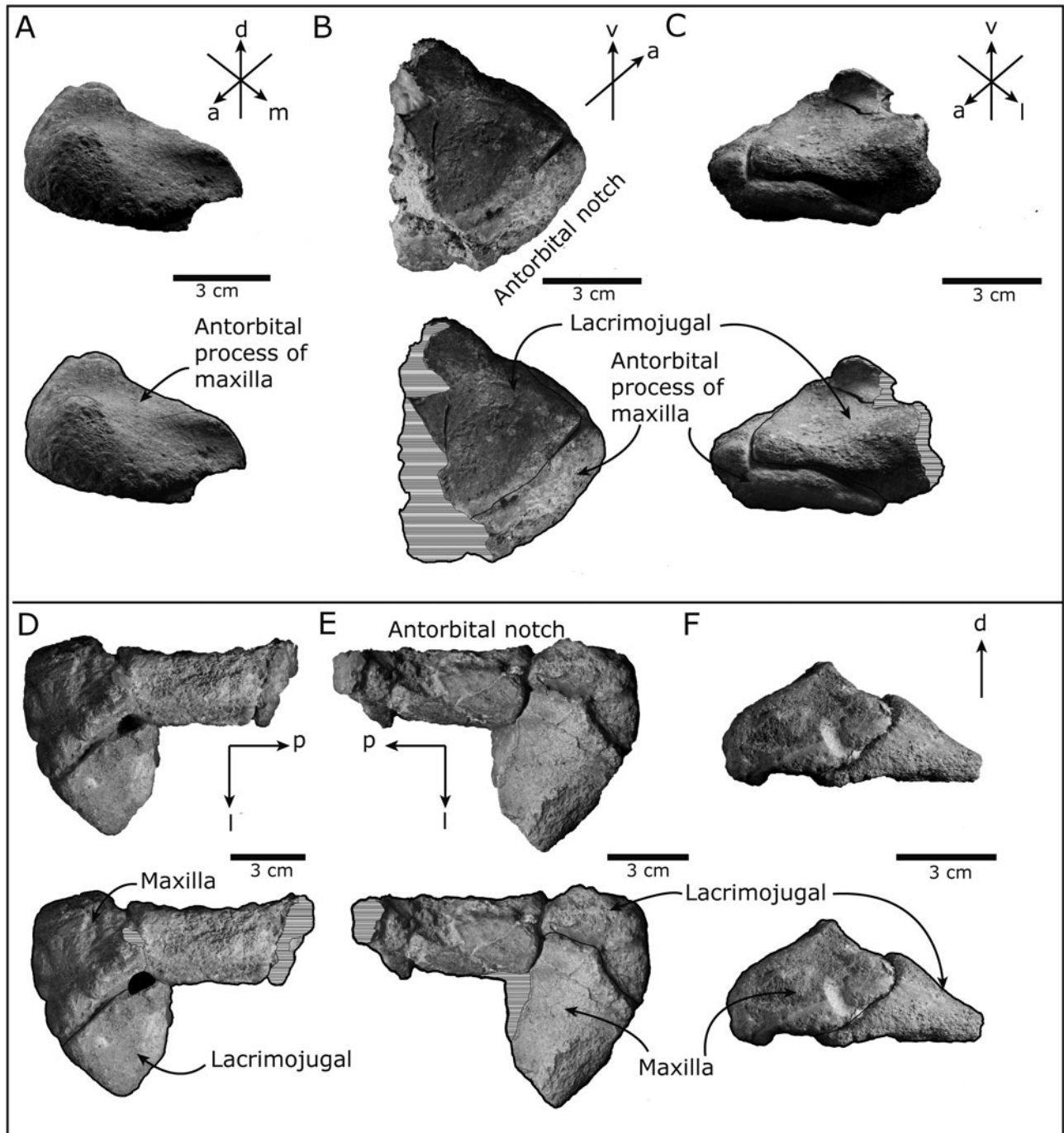
Figure 4. Fragments of the holotype cranium of *Diaphorocetus poucheti* (MLP 5-6). **A,** right antorbital process of the maxilla in dorsal view; **B,** right antorbital process of the maxilla with lacrimojugal in ventral view; **C,** right antorbital process of the maxilla with lacrimojugal in lateral view; **D,** left antorbital process of the maxilla with lacrimojugal in ventral view; **E,** left antorbital process of the maxilla with lacrimojugal in dorsal view; **F,** left antorbital process of the maxilla with lacrimojugal in anterior view. Hatched areas indicate broken and eroded surfaces.

triangular and oriented posteromedially. In lateral view, the exoccipital is oriented obliquely relative to the horizontal plane. The occipital condyles are strongly convex, situated on a short neck and oriented posterodorsally; compared to *Physeter*, they are located more ventrally relative to the occipital shield. In dorsal view, the exoccipital contacts the squamosal along a semicircular suture.
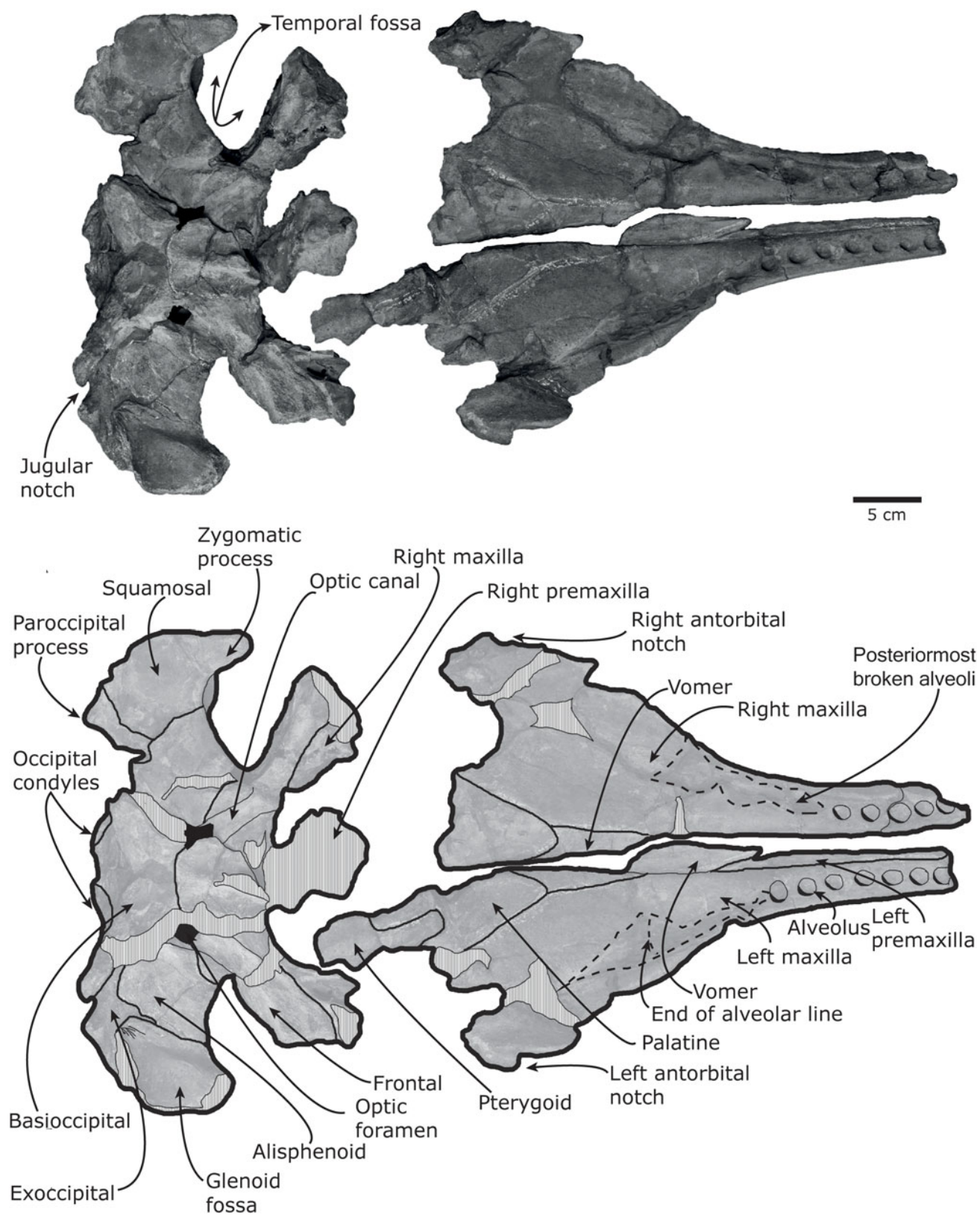
Figure 5. Holotype cranium of *Diaphorocetus poucheti* (MLP 5-6) in ventral view. **A,** photograph; **B,** explanatory line drawing. Hatched areas indicate broken and eroded surfaces; dark shading indicates natural cavities; stippled lines denote incomplete parts.
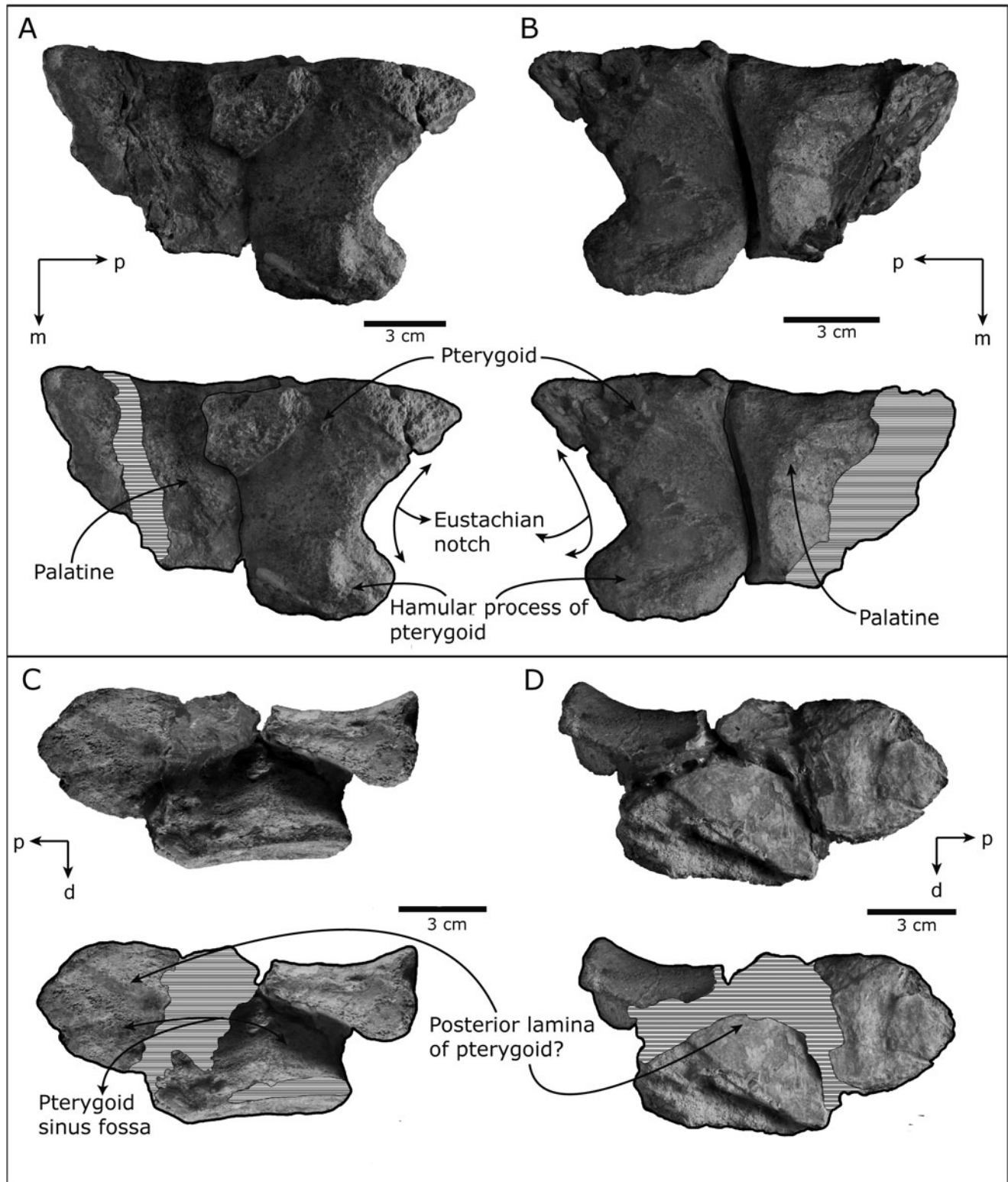
Figure 6. Fragments of the holotype cranium of *Diaphorocetus poucheti* (MLP 5-6). **A,** right palatine and pterygoid in ventral view; **B,** right palatine and pterygoid in dorsal view; **C,** part of the left pterygoid in medial view; **D,** part of the left pterygoid in lateral view. Hatched areas indicate broken and eroded surfaces.
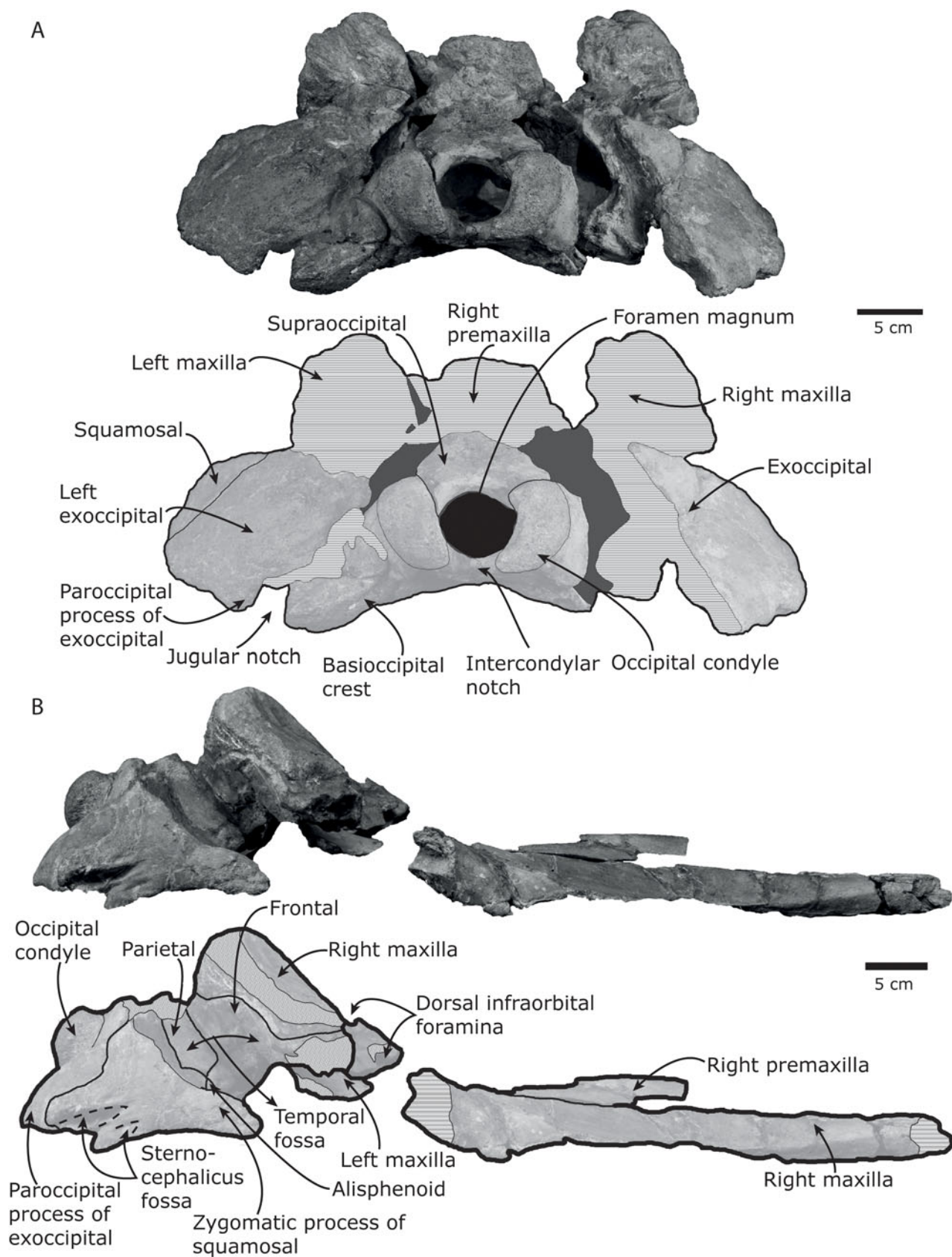
A

B

Figure 7. Holotype cranium of *Diaphorocetus poucheti* (MLP 5-6) in (**A**) dorsal and (**B**) right lateral view. Light shading indicates missing parts; hatched areas indicate broken and eroded surfaces; dark shading indicates natural cavities.
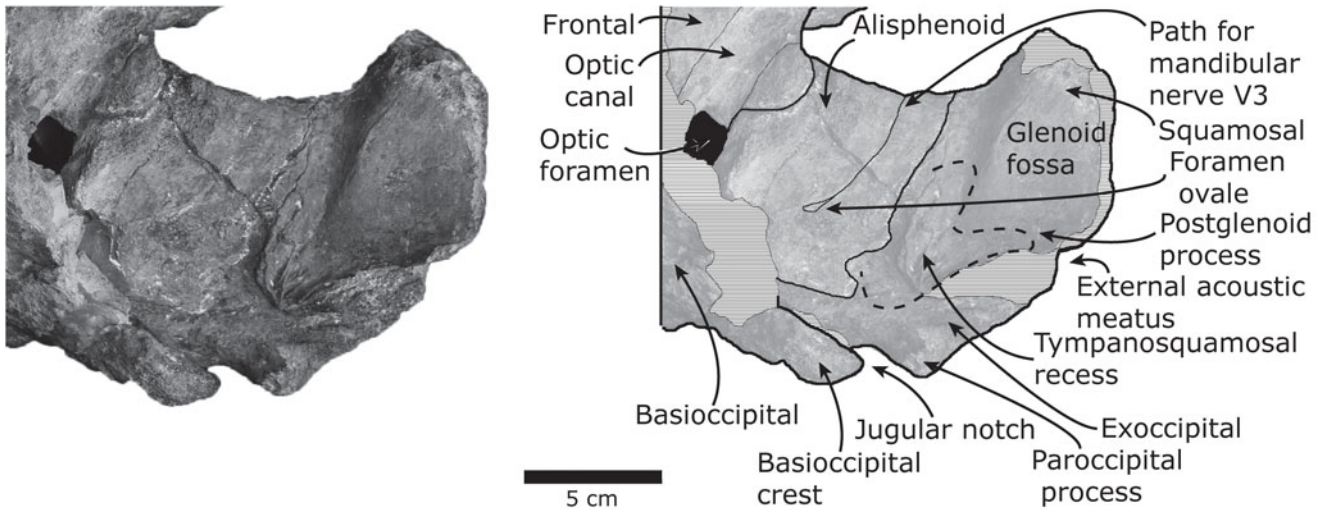
Figure 8. Left basicranium of the holotype of *Diaphorocetus poucheti* (MLP 5-6) in ventral view. **A,** photograph; **B,** explanatory line drawing. Hatched areas indicate broken and eroded surfaces; dark shading indicates natural cavities; stippled lines delimit the tympanosquamosal recess.

Squamosal. The squamosal is better preserved on the right. In lateral view, the zygomatic process is triangular, longer than high and terminates in a rounded and ventrally deflected apex (Fig. 7B). The seemingly ventral orientation of the zygomatic process is unusual and partly (but not entirely) may reflect post-mortem deformation and errors in the original mounting of the skull. The postglenoid process is relatively thin and oriented posteriorly. Posterodorsal to this process, there are two deep fossae, presumably for the sternocephalicus and brachiocephalicus muscles. On the medial wall of the temporal fossa, the squamosal contacts the alisphenoid along a dorsally convex, irregular suture (Fig. 7B).

In dorsal view, the zygomatic process is oriented anteriorly and delimits the posterior two-thirds of the temporal fossa. There is a well-developed supramastoid crest. In ventral view, the glenoid fossa is shallow and posteriorly delimited by the slightly twisted postglenoid process (Fig. 8). The external acoustic meatus is wide, shallow, oriented laterally and posteriorly bordered by a postympanic process. The tympanosquamosal recess is shallow, wider than long and poorly defined. The falciform and spiny processes are broken and missing on both sides (Fig. 8).

Alisphenoid. In ventral view, the alisphenoid is approximately square (Fig. 5) and one of the most conspicuous bones of the basicranium. The foramen ovale is poorly preserved and obscured by sediment but appears to be small and gives rise to a shallow, semicircular path for the mandibular nerve (Fig. 8). The alisphenoid contacts the frontal anteromedially (along an 'S'-shaped suture), the squamosal posterolaterally (along an approximately

straight suture), the posterior lamina of the pterygoid posteromedially, and the exoccipital and, probably, the basioccipital posteriorly. In lateral view, a small portion of the alisphenoid is exposed on the ventromedial wall of the temporal fossa, where it contacts the squamosal (Fig. 7B).
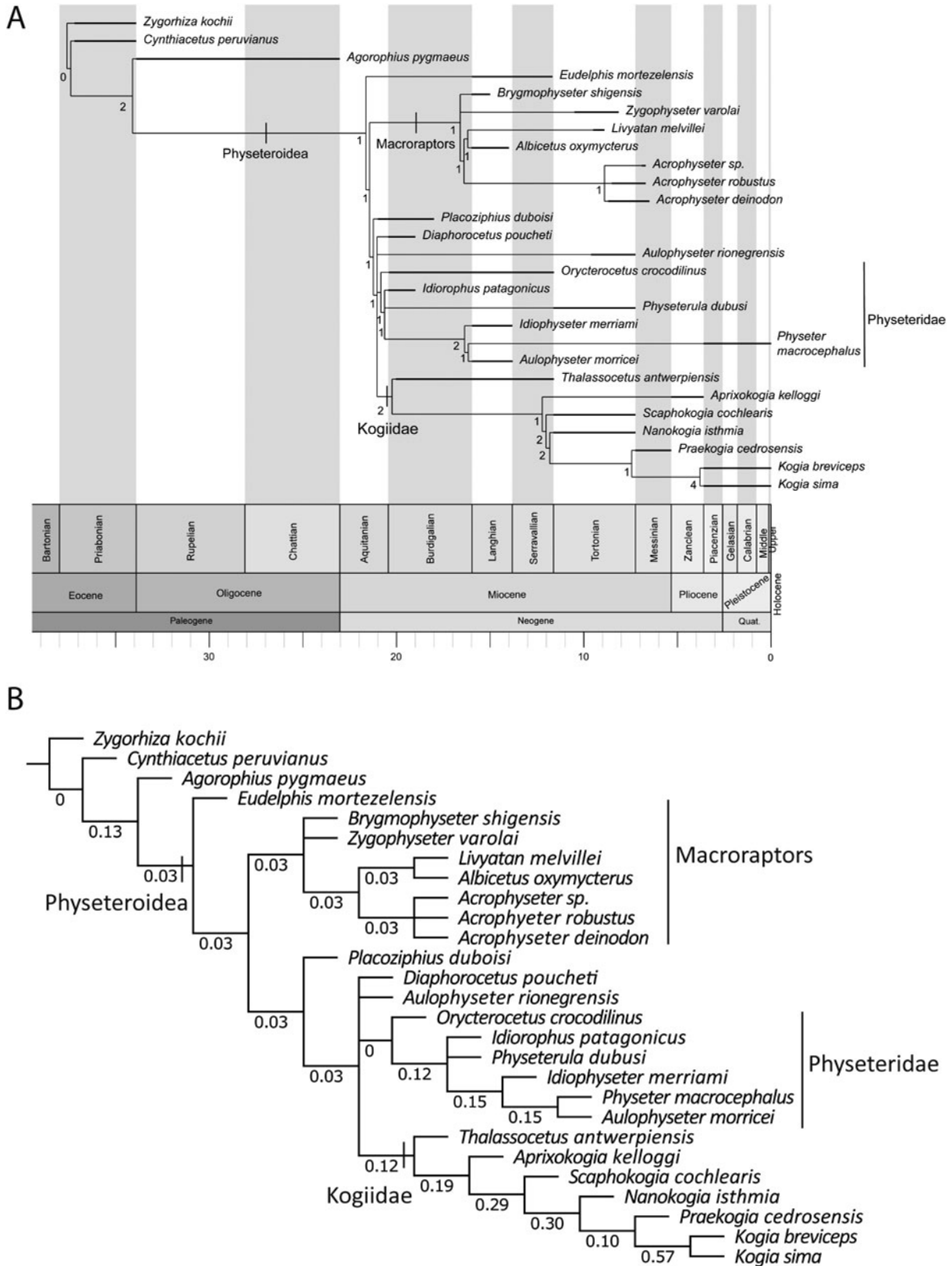
Basioccipital. The basioccipital is fused to the basisphenoid, with no visible suture remaining. The basioccipital crest is robust, elongate and oriented posterolaterally (Fig. 5); in posterior view, it is oriented ventrolaterally and forms an acute angle (45°) with the sagittal plane.

Supraoccipital. Only a small portion of the supraoccipital is preserved. In lateral view, it is oriented at an angle of approximately 60° relative to the horizontal plane.

Phylogenetic analysis

Equally weighted morphological analysis

The equally weighted analysis resulted in four MPTs with lengths of 153 steps (consistency index [CI] = 0.536; retention index [RI] = 0.732). The strict consensus tree is relatively well resolved, even though branch support is generally low (Fig. 9A). *Eudelphis* is the basal-most physeteroid and sister to two major subclades. The first of these comprises the macroraptorial species *Acrophyseter* spp., *Albicetus*, *Brygmophyseter*, *Livyatan* and *Zygophyseter*, and is supported by the presence of two large dorsal infraorbital foramina in the vicinity of the right antorbital notch (char. 12); dental roots with a transverse diameter >5% of the

Figure 9. **A,** time-calibrated strict consensus of the four most parsimonious trees (MPTs) resulting from the cladistic analysis under equal weights; **B,** strict consensus of the two MPTs resulting from the cladistic analysis under implied weights (k = 3). Numbers associated with branches are Bremer decay values. Temporal ranges are specified in Supplementary material 1, Appendix 4.

bizygomatic width (char. 37); and a convex lateral margin of the atlas giving rise to a centrally located, horizontal transverse process (char. 53).

The second major subclade is defined by the reduction of the falciform process (char. 32) and the position of the posterior-most upper alveolus near the antorbital notch (char. 42), and recovers *Placoziphius* as sister to a polytomy comprising *Diaphorocetus*, '*Aulophyseter*' rionegrensis and the two crown lineages, Physeteridae (including *Aulophyseter morricei*, *Idiophyseter*, *Idiorophus*, *Orycterocetus crocodilinus*, *Physeter* and *Physeterula*) and Kogiidae (including *Aprixokogia*, *Kogia* spp., *Nanokogia*, *Praekogia*, *Scaphokogia* and *Thalassocetus*). The exact position of *Diaphorocetus* within this group remains ambiguous.

Diaphorocetus and '*Aulophyseter*' rionegrensis share with physeterids and kogiids a low ($\leq$0.20) ratio between the width of the premaxillary foramen and the width of the premaxilla (char. 17). *Diaphorocetus* further shares with physeterids and kogiids the small size of the temporal fossa (char. 26), relatively small teeth (char. 37) and the position of the last upper alveolus notably anterior to the antorbital notch (char. 42). Nevertheless, *Diaphorocetus* also shows an archaic trait absent in '*A.*' rionegrensis that may suggest a more basal position: deep upper alveoli (char. 7).

The IterPCR procedure (Pol & Escapa 2009; Escapa & Pol 2011) identified both *Diaphorocetus* and '*Aulophyseter*' rionegrensis as unstable (Supplementary material 1, Appendix 3), but placed the former always in a crownward position, either as the sister to Physeteridae (two MPTs) or as sister to Kogiidae (two MPTs; one synapomorphy: postorbital process extended ventrally, char. 44).

Physeterids are defined by two unambiguous synapomorphies: a flat or concave, vertically oriented occipital shield (char. 31); and a short, rounded contact between the jugal and the zygomatic process of the squamosal (char. 47). Further, there are two ambiguous synapomorphies: the size of the temporal fossa (char. 26); and a short superior process of the periotic extending beyond the medial margin of the internal acoustic meatus (char. 49). Kogiids are completely resolved and supported by two unambiguous synapomorphies: a maximum bizygomatic width of <40 cm (char. 9); and the presence of a sagittal crest in the form of a shelf covered by the pointed right premaxilla (char. 15). Again, there are also two ambiguous synapomorphies: the extension of the right maxilla to the sagittal plane on the posterior wall of the supracranial basin (char. 21); and the presence of a ventrally extended postorbital process of the frontal, in conjunction with a low position of the zygomatic process of the squamosal (character 44).

Implied weighting. The analysis under implied weights (k = 3) resulted in two MPTs (fit = 13.97143). The strict consensus matches that of the equally weighted analysis (Fig. 9B), but with slightly improved support for Physeteridae (See Supplementary material 1, Appendix 3 for results based on other k values).

Discussion

Phylogenetic implications
As one of the oldest sperm whales, *Diaphorocetus* is key to understanding the early evolutionary history of physeteroids and demonstrates that pronounced facial asymmetry and a clearly defined supracranial basin have characterized this lineage since at least the early Miocene (*c.* 20 Ma). We consistently recovered *Diaphorocetus* in a relatively crownward position (in contrast to Bianucci & Landini 2006 and Lambert *et al.* 2008), without, however, being able to determine its precise relationships. Its peculiar combination of derived and archaic traits, poor state of preservation and lack of ear bones currently prevent a more confident assessment of its phylogenetic affinities. Recovery of additional material and/or a revaluation of other Patagonian physeteroids – in particular, '*Aulophyseter*' rionegrensis – may help to resolve this situation.

Our analysis is the first to recover all macroraptorial sperm whales as a clade, suggesting that their distinctive feeding adaptations (Lambert *et al.* 2016) may have a common evolutionary origin. Plotting our phylogeny against time (Fig. 9A) furthermore reveals three major ghost lineages: one (*c.* 7 Ma) leading to the macroraptorial clade; one (*c.* 4 Ma) leading to the physeterid subclade comprising *Aulophyseter morricei*, *Idiophyseter* and *Physeter*; and one separating the uncertainly dated *Thalassocetus* (Lambert 2008) from the remainder of Kogiidae. In addition to these ghost lineages, our time-calibrated phylogeny implies major range extensions for *Physeter* and '*Aulophyseter*' rionegrensis. The latter is likely an artefact of the polytomy at (or just below) the base of the clade formed by *Diaphorocetus*, '*Aulophyseter*' rionegrensis, Physeteridae and Kogiidae, and may be resolved following a reassessment of other early Miocene physeteroids from Patagonia. The lack of Miocene fossils of *Physeter* might be related to its deep-sea habitat.

Overall, our results support a middle–late Miocene diversification of physeteroids, which started around 16 Ma and involved *Eudelphis*, macroraptorial sperm whales and some members of the crown group (i.e. *Aulophyseter*, *Idiophyseter*, *Physeterula*, *Nanokogia*, *Praekogia* and *Scaphokogia*). Considering the notable

disparity of the taxa involved, as expressed in their variable body size and tooth morphology, it is tempting to speculate that this radiation may have been related to the exploitation of different ecological niches (Velez-Juarbe *et al.* 2015).

Palaeobiology of *Diaphorocetus*

Evolution of body size. Extant sperm whales differ remarkably in length, with *Physeter macrocephalus* reaching 12 m (in females) or 18 m (in males), whereas *Kogia* spp. only grows to 2–3.5 m. As elsewhere in South America (Lambert *et al.* 2010, 2016; Collareta *et al.* 2017), Patagonian Miocene physeteroids comprise a disparate assemblage of small to medium-sized (*Diaphorocetus*, '*Aulophyseter*', *Idiorophus*) and large (*Livyatan*; Piazza *et al.* 2018) species. Globally, however, early Miocene physeteroids never exceeded 6 m in length. In Patagonia, *Diaphorocetus* occurred at broadly the same time as the somewhat larger *Idiorophus*, suggesting the presence of two different ecomorphs.

Large sperm whales first appeared during the middle Miocene, possibly as a result of independent trends in stem and crown physeteroids (Boersma & Pyenson 2015; Lambert *et al.* 2016). Optimizing body length on our phylogeny supports this idea, with gigantism arising independently in the macroraptorial clade and physeterids. Large body size across odontocetes has been correlated with a squid-based diet (Slater *et al.* 2010). This idea is difficult to apply to physeteroids, given that: (i) large size seems to have accompanied raptorial feeding in several stem taxa (Bianucci & Landini 2006; Lambert *et al.* 2010, 2014); and (ii) extant kogiids are small, yet mostly feed on cephalopods. Overall, the evolution of physeteroid body size likely followed a more complex pattern, which may be elucidated through ecomorphological information gleaned from both extant taxa and the fossil record.

Feeding strategy. Living sperm whales capture their prey via suction, which involves the generation of negative pressure inside the oral cavity via rapid movements of the tongue and hyoid (Werth 2000, 2004). This strategy is reflected in a range of anatomical specializations, such as a lack of upper teeth, well-developed gular musculature and a small temporal fossa (Werth 2000, 2004, 2006; Johnston & Berta 2011). Nevertheless, kogiids and physeterids differ notably in the way that they generate suction: whereas the former rely on their blunt and short rostrum, in the latter prey is drawn directly into the oropharynx via movements of the short and caudally positioned tongue (Werth 2004).

In contrast to their extant relatives, many stem physeteroids likely were macroraptorial and perhaps even preyed on other marine mammals. Features traditionally associated with this feeding style include robust upper and lower teeth, a large temporal fossa housing well-developed jaw muscles, an elongate zygomatic process of the squamosal, a relatively long rostrum and a robust mandible (Bianucci & Landini 2006; Lambert *et al.* 2016).

The morphology of *Diaphorocetus* appears intermediate between that of macroraptorial physeteroids and their extant, suction feeding relatives. Unlike in *Physeter* and *Kogia*, its upper teeth are deeply rooted and separated by wide interalveolar septa; yet they are smaller than those in clearly macroraptorial forms (see Supplementary material 1, Appendix 3). Its temporal fossa is proportionately smaller than that of *Acrophyseter* and *Zygophyseter*, yet larger than that of *Physeter*. Finally, it has an elongate zygomatic process and bottleneck-like rostrum as in *Acrophyseter* and *Zygophyseter*, yet also a tooth row that terminates far anterior to the antorbital notch (in contrast to macroraptorial forms; Supplementary material 1, Appendix 3).

The mosaic nature of its feeding apparatus suggests that *Diaphorocetus* may have employed an intermediate range of behaviours, for example capturing small prey (e.g. fish) with its teeth, before sucking them towards the back of the oral cavity for swallowing (Werth 2006; Hocking *et al.* 2017). Similar feeding behaviour occurs in some extant delphinids, such as *Lagenorhynchus* (Kane & Marshall 2009).

Evolution of the spermaceti organ and junk. All sperm whales are characterized by the presence of a supracranial basin housing the spermaceti organ and junk. There are several hypotheses as to the function of the spermaceti organ (see Huggenberger *et al.* 2016), ranging from echolocation (Norris & Harvey 1972; Heyning 1989; Heyning & Mead 1990) to buoyancy control (Clarke 1979), sexual dimorphism and intra-male fighting (Cranford 1999; Carrier *et al.* 2002), and/or the reduction of air pressure during dives (Schenkkan & Purves 1973). Today, the first hypothesis is the most accepted, although the others remain possible.

The evolution, size and shape of the spermaceti organ in extinct physeteroids can be inferred from the supracranial basin. Its size and development vary, with the basin in its most extensive form extending along the rostrum (in *Physeter* and *Livyatan*) and/or the orbital region (in *Acrophyseter deinodon* and *Zygophyseter*). In *Diaphorocetus*, the dorsal surface of the rostrum is convex, rather than concave as in *Physeter* and *Livyatan*, suggesting that the basin did not extend beyond the neurocranium.

Posteriorly, the supracranial basin of *Diaphorocetus* is limited by the obliquely oriented supraoccipital shield
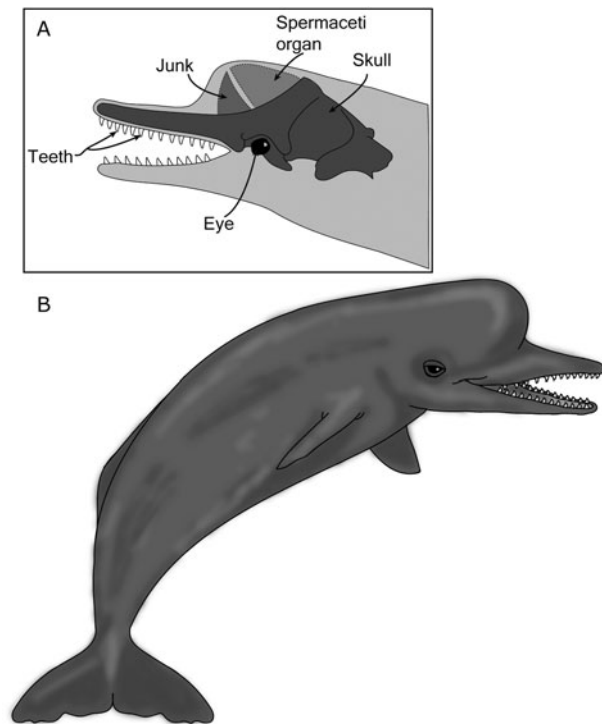
Figure 10. Schematic reconstruction of *Diaphorocetus poucheti*. **A,** head in lateral view showing the nasal complex and proposed outline of spermaceti organ and junk, based on *Zygophyseter varolai* Bianucci & Landini, 2006; **B,** full body reconstruction. Drawing by Florencia Paolucci.

(Fig. 10A), suggesting that its spermaceti organ was comparatively small (Fig. 10B). This condition is shared with *Eudelphis*, *Placoziphius* and, probably, *Aulophyseter morricei*, and again notably contrasts with the better developed supracranial basin of other Miocene physeteroids, such as *Livyatan* and *Zygophyseter*. Externally, the spermaceti organ and junk of *Diaphorocetus* may have appeared hemispherical, as previously proposed for *Zygophyseter* (Bianucci *et al.* 2006). They would, however, likely have been smaller and lower, thus giving the rostrum the appearance of an elongate beak (Fig. 10).

Conclusions

Diaphorocetus is one of two small to medium-sized sperm whale ecomorphs that inhabited the early Miocene waters off Patagonia. It represents one of the oldest physeteroids and demonstrates that facial asymmetry and a clearly defined supracranial basin have characterized this lineage for at least 20 Ma. Judging from the size and extent of the supracranial basin, the spermaceti organ and junk of *Diaphorocetus* were comparatively small. Its feeding apparatus appears consistent with both raptorial and suction feeding, likely enabling the capture of small prey via a combination of the two. Our phylogenetic analysis supports the hypothesis that gigantism arose more than once during sperm whale evolution.

Acknowledgements

Supplemental material

Supplementary material for this article can be accessed at: https://doi.org/10.1080/14772019.2019.1605544.

ORCID

Florencia Paolucci http://orcid.org/0000-0003-4466-7723
Marta S. Fernández http://orcid.org/0000-0001-6935-7575

References

Allen, G. M. 1921. Fossil cetaceans from the Florida phosphate beds. *Journal of Mammalogy*, **2**(3), 144–159.
Ameghino, F. 1894a. Enumération synoptique des espèces de mammifères fossiles des formations éocènes de Patagonie. *Boletin de la Academia Nacional de Ciencias en Córdoba*, **13**, 259–455.
Ameghino, F. 1894b. Sur les ongulés fossiles de l'Argentine (Examen critique de l'ouvrage de R. Lydekker: a study of the extinct ungulates of Argentina). *Revista del jardín Zoológico de Buenos Aires*, **2**(7), 193–224.
Ameghino, F. 1921. Primera sinopsis Geológico Paleontológica: Notas sobre cuestiones de geología y paleontología argentinas. Pp. 1–767 in A. J. Torcelli (ed.)

Obras completas y correspondencia científica de Florentino Ameghino. Volume 12. La Plata, Taller de Impresiones Oficiales.

Bianucci, G. & **Landini, W.** 1999. *Kogiapusilla* from the middle Pliocene of Tuscany (Italy) and a phylogenetic analysis of the family Kogiidae (Odontoceti, Cetacea). *Rivista Italiana di Paleontologia e Stratigrafia*, **105**, 445–453.

Bianucci, G. & **Landini, W.** 2006. Killer sperm whale: a new basal physeteroid (Mammalia, Cetacea) from the late Miocene of Italy. *Zoological Journal of the Linnean Society*, **148**(1), 103–131.

de Blainville, H.. 1838. Sur les cachalots. *Annales Françaises Étrangères de Anatomie et Physiologie*, **2**, 335–337.

Boersma, A. T. & **Pyenson, N. D.** 2015. *Albicetus oxymycterus*, a new generic name and redescription of a basal physeteroid (Mammalia, Cetacea) from the Miocene of California, and the evolution of body size in sperm whales. *PLoS ONE*, **10**(12), e0135551. https://doi.org/10.1371/journal.pone.0135551

Brisson, M. J. 1762. *Regnum animale in classes IX distributum, sive, synopsis methodical sistens generalem animalium distributionem in classes IX, & duarum primarum classius, quadrupedum scilicet & cetaceorum, particularem divisionem in ordines, sectiones, genera & species, cum brevi cujusque speciei, description, citationibus auctorum de iis tractantium, nominibus eis ab ipsis & nationibus impositis, nomini busque vulgaribus*. Editio altera auctior. Second Edition. Theodorum Haak, Lugduni Batavorum, Leiden, 296 pp.

Buono, M. R. 2014. *Evolución de los Balaenidae (Mammalia, Cetacea, Mysticeti) del Mioceno de Patagonia: sistemática, filogenia y aspectos paleobiológicos*. Unpublished PhD thesis, Facultad de Ciencias Naturales y Museo, Universidad Nacional de La Plata, 324 pp.

Buono, M. R., **Fernández, M. S.**, **Cozzuol, M. A.**, **Cuitiño, J. I.** & **Fitzgerald, E. M.** 2017. The early Miocene balaenid *Morenocetus parvus* from Patagonia (Argentina) and the evolution of right whales. *PeerJ*, **5**, e4148. https://doi.org/10.7717/peerj.4148

Cabrera, A. 1926. Cetáceos fósiles del Museo de La Plata. *Revista del Museo de La Plata*, **29**, 363–411.

Canto, J. 2007. Registros de Physeteroidea (Cetacea: Odontoceti) fósiles para Chile. *Noticiario Mensual del Museo Nacional de Historia Natural (Chile)*, **359**, 9–22.

Carrier, D. R., **Deban, S. M.** & **Otterstrom, J.** 2002. The face that sank the Essex: potential function of the spermaceti organ in aggression. *Journal of Experimental Biology*, **205**, 1755–1763.

Clarke, M. R. 1979. The head of the sperm whale. *Scientific American*, **240**(1), 128–141.

Cione, A. L., **Cozzuol, M. A.**, **Dozo, M. T.** & **Acosta Hospitaleche, C.** 2011. Marine vertebrate assemblages in the southwest Atlantic during the Miocene. *Biological Journal of the Linnean Society*, **103**, 423–440.

Coddington, J. & **Scharff, N.** 1994. Problems with zero-length branches. *Cladistics*, **10**(4), 415–423.

Collareta, A., **Lambert, O.**, **De Muizon, C.**, **Urbina, M.** & **Bianucci, G.** 2017. *Koristocetus pescei* gen. et sp. nov., a diminutive sperm whale (Cetacea: Odontoceti: Kogiidae) from the late Miocene of Peru. *Mitteilungenausdem Museum für Naturkunde in Berlin (Fossil Record)*, **20**(2), 259.

Cope, E. D. 1895. Fourth contribution to the marine fauna of the Miocene period of the United States. *Proceedings of the American Philosophical Society*, **34**(147), 135–155.

Cozzuol, M. A. 1993. *Mamíferos acuáticos del mioceno medio y tardío en Argentina: sistemática, evolución y biogeografía*. Unpublished PhD thesis, Facultad de Ciencias Naturales y Museo, Universidad Nacional de La Plata, 175 pp.

Cozzuol, M. A. 1996. The record of the aquatic mammals in southern South America. *Munchner Geowissenschaftliche Abhandlungen*, **30**, 321–342.

Cranford, T. W. 1999. The sperm whale's nose: sexual selection on a grand scale? *Marine Mammal Science*, **15**, 1133–1157.

Cranford, T. W., **Amundin, M.** & **Norris, K. S.** 1996. Functional morphology and homology in the Odontocete nasal complex: implications for sound generation. *Journal of Morphology*, **228**, 223–285.

Cuitiño, J. I., **Dozo, M. T.**, **del Río, C. J.**, **Buono, M. R.**, **Palazzesi, L.**, **Fuentes, S.** & **Scasso, R. A.** 2017. Miocene marine transgressions: paleoenvironments and paleobiodiversity. Pp. 47–84 in P. Bouza & A. Bilmes (eds) *Late Cenozoic of Península de Valdés, Patagonia, Argentina: An Interdisciplinary Approach*. Springer Earth System Sciences, Springer International Publishing AG, Cham.

Escapa, I. H. & **Pol, D.** 2011. Dealing with incompleteness: new advances for the use of fossils in phylogenetic analysis. *Palaios*, **26**(3), 121–124.

Flower, W. H. 1867. IV. Description of the skeleton of *Inia geoffrensis* and of the skull of *Pontoporia blainvillii*, with remarks on the systematic position of these animals in the Order Cetacea. *Journal of Zoology*, **6**(3), 87–116.

Flower, W. H. 1868. On the osteology of the cachalot or sperm whale (*Physeter macrocephalus*). *Transactions of the Zoological Society of London*, **6**, 309–372.

Fordyce, R. E. 2009. Cetacean fossil record. Pp. 207–215 in W. F. Perrin, B. Würsig & J. G. M. Thewissen (eds) *Encyclopedia of marine mammals*. Second Edition. Academic Press, San Diego.

Fordyce, R. E. & **Muizon, C. de.** 2001. Evolutionary history of cetaceans: a review. Pp. 169–233 in J.-M. Mazin & V. de Buffrenil (eds) *Secondary adaptations of tetrapods to life in water*. Verlag Dr Friederich Pfeil, Munich.

Galatius, A. 2009. Paedomorphosis in two small species of toothed whales (Odontoceti): how and why? *Biological Journal of the Linnean Society*, **99**, 278–295.

Goloboff, P. A., **Farris, J. S.** & **Nixon, K. C.** 2008a. TNT, a free program for phylogenetic analysis. *Cladistics*, **24**(5), 774–786.

Goloboff, P. A., **Carpenter, J. M.**, **Arias, J. S.** & **Esquivel, D. R. M.** 2008b. Weighting against homoplasy improves phylogenetic analysis of morphological data sets. *Cladistics*, **24**(5), 758–773.

Gray, J. E. 1821. On the natural arrangement of vertebrose animals. *London Medical Repository*, **15**, 296–310.

Haller, M. J., **Meister, C. M.**, **Monti, A. J.** & **Weiler, N.** 2005. Hoja Geológica 4366-II Puerto Madryn Servicio Geológico Minero Argentino. *Boletín*, **289**, 1–40.

Hampe, O. 2006. Middle/late Miocene hoplocetine sperm whale remains (Odontoceti: Physeteridae) of North Germany with an emended classification of the Hoplocetinae. *Fossil Record*, **9**(1), 61–86.

Heyning, J. E. 1989. Comparative facial anatomy of beaked whales (Ziphiidae) and a systematic revision among the families of extant Odontoceti. *Contributions in Science, Natural History Museum of Los Angeles County*, **405**, 1–64.

Heyning, J. E. 1997. Sperm whale phylogeny revisited: analysis of the morphological evidence. *Marine Mammal Science*, **13**, 596–613.

Heyning, J. E. & Mead, J. G. 1990. Evolution of the nasal anatomy of cetaceans. Pp. 67–80 in J. A. Thomas & R. A. Kastelein (eds) *Sensory abilities of cetaceans*. Springer, Boston, MA.

Hirota, K. & Barnes, L. G. 1994. A new species of middle Miocene sperm whale of the genus *Scaldicetus* (Cetacea; Physeteridae) from Shiga-Mura, Japan. *The Island Arc*, **3**, 453–472.

Hocking, D. P., Marx, F. G., Park, T., Fitzgerald, E. M. G. & Evans, A. R. 2017. A behavioural framework for the evolution of feeding in predatory aquatic mammals. *Proceedings of the Royal Society B*, **284**, 20162750. https://doi.org/10.1098/rspb.2016.2750

Huggenberger, S., André, M. & Oelschläger, H. H. 2016. The nose of the sperm whale: overviews of functional design, structural homologies and evolution. *Journal of the Marine Biological Association of the United Kingdom*, **96**(4), 783–806.

Johnston, C. & Berta, A. 2011. Comparative anatomy and evolutionary history of suction feeding in cetaceans. *Marine Mammal Science*, **27**, 493–513.

Kane, E. A. & Marshall, C. D. 2009. Comparative feeding kinematics and performance of odontocetes: belugas, Pacific white-sided dolphins and long-finned pilot whales. *Journal of Experimental Biology*, **212**, 3939–3950. https://doi.org/10.1242/jeb.034686

Kázar, E. 2002. Revised phylogeny of the Physeteridae (Mammalia: Cetacea) in the light of *Placoziphius* Van Beneden, 1869 and *Aulophyseter* Kellogg, 1927. *Bulletin de l'Institut Royal des Sciences Naturelles de Belgique, Sciences de la Terre*, **72**, 151–170.

Kellogg, R. 1925. Two fossil physeteroid whales from California. *Contributions to Palaeontology from the Carnegie Institution of Washington*, **348**, 1–34.

Kellogg, R. 1928. The history of whales – their adaptation to life in the water. *The Quarterly Review of Biology*, **3**(1), 29–76.

Kellogg, R. 1965. Fossil marine mammals from the Miocene Calvert Formation of Maryland and Virginia. The Miocene Calvert sperm whale *Orycterocetus*. *Bulletin of the United States National Museum*, **247**, 47–63.

Kimura, T. & Hasegawa, Y. 2006. Fossil sperm whales (Cetacea, Physeteridae) from Gunma and Ibaraki prefectures, Japan; with observations on the Miocene fossil sperm whale *Scaldicetus shigensis* Hirota and Barnes, 1995. *Bulletin of the Gunma Museum of Natural History*, **10**, 1–23.

Lambert, O. 2008. Sperm whales from the Miocene of the North Sea: a re-appraisal. *Bulletin de l'Institut Royal des Sciences Naturelles de Belgique, Sciences de la Terre*, **78**, 277–316.

Lambert, O., Bianucci, G. & Beatty, B. L. 2014. Bony outgrowths on the jaws of an extinct sperm whale support macroraptorial feeding in several stem physeteroids. *Naturwissenschaften*, **101**, 517–521.

Lambert, O., Bianucci, G. & de. Muizon, C. 2008. A new stem-sperm whale (Cetacea, Odontoceti, Physeteroidea) from the latest Miocene of Peru. *Comptes Rendus Palevol*, **7**(6), 361–369.

Lambert, O., Bianucci, G. & Muizon, C. de. 2016. Macroraptorial sperm whales (Cetacea, Odontoceti, Physeteroidea) from the Miocene of Peru. *Zoological Journal of the Linnean Society*, **179**(2), 404–474.

Lambert, O., Bianucci, G., Post, K., de Muizon, C., Salas-Gismondi, R., Urbina, M. & Reumer, J. 2010. The giant bite of a new raptorial sperm whale from the Miocene epoch of Peru. *Nature*, **466**, 105–108.

Linnaeus, C. 1758. *Systema naturae per regna trianaturae, secundum classes, ordines, genera, species, cum characteribus, differentiis, synonymis, locis. Volume 1* [Tenth Edition]. Holmiae, Stockholm, 824 pp.

Lydekker, R. 1893 [1894]. Cetacean skulls from Patagonia. *Anales del Museo de la Plata*, **2**, 1–13.

McGowen, M. R., Spaulding, M. & Gatesy, J. 2009. Divergence date estimation and a comprehensive molecular tree of extant cetaceans. *Molecular Phylogenetics and Evolution*, **53**(3), 891–906.

Mchedlidze, G. A. 1970. *Some general characteristics of the evolution of cetaceans*. Akademia Nauk Gruzinskoi S.S.R., Institut Paleobiologii, Tbilisi, 1, pp. 1–112.

Mchedlidze, G. A. 2009. Sperm whales, evolution. Pp. 1097–1098 in W. F. Perrin, B. Würsig & J. G. M. Thewissen (eds) *Encyclopedia of marine mammals*. Second Edition. Academic Press, San Diego.

Mead, J. G. & Fordyce, R. E. 2009. The therian skull: a lexicon with emphasis on the odontocetes. *Smithsonian Contributions to Zoology*, **627**, 1–248.

Moreno, F. P. 1892. Lijeros apuntes sobre dos generos de cetaceos fosiles de la Republica Argentina. *Revista de la Museo La Plata*, **3**, 393–400.

de Muizon, C.. 1991. A new Ziphiidae (Cetacea) from the early Miocene of Washington State (USA) and phylogenetic analysis of the major groups of odontocetes. *Bulletin du Muséum National d'Histoire Naturelle. Section C, Sciences de la terre, paléontologie, géologie, minéralogie*, **12**(3–4), 279–326.

Norris, K. S. & Harvey, G. W. 1972. A theory for the function of the spermaceti organ of the sperm whale (*Physeter catodon* L.). *NASA Special Publications*, **262**, 397–417.

Owen, R. 1866. On some Indian Cetacea collected by Walter Elliot, Esq. *Transactions of the Zoological Society of London*, **6**, 17–47.

Pérez, L. M., Cione, A. L., Cozzuol, M. & Varela, A. N. 2011. A sperm whale (Cetacea: Physeteroidea) from the Paraná Formation (late Miocene) of Entre Ríos, Argentina. Environment and taphonomy. *Ameghiniana*, **48**, 648–654.

Perrin, W. F. 1975. Variation of spotted and spinner porpoise (genus *Stenella*) in the eastern Pacific and Hawaii. *Scripps Institution of Oceanography*, **21**, 206.

Piazza, D. S., Agnolin, F. L. & Lucero, S. 2018. First record of a macroraptorial sperm whale (Cetacea, Hyseteroidea) from the Miocene of Argentina. *The Journal of the Brazilian Society of Paleontology*, **21**(3), 276–280.

Pol, D. & Escapa, I. H. 2009. Unstable taxa in cladistic analysis: identification and the assessment of relevant characters. *Cladistics*, **25**(5), 515–527.

Pyenson, N. D. & Sponberg, S. N. 2011. Reconstructing body size in extinct crown Cetacea (Neoceti) using

allometry, phylogenetic methods and tests from the fossil record. *Journal of Mammalian Evolution*, **18**(4), 269–288.

Raven, H. C. & Gregory, W. K. 1933. The spermaceti organ and nasal passages of the sperm whale (*Physeter catodon*) and other odontocetes. *American Museum Novitates*, **677**, 1–18.

Schenkkan, E. J. & Purves, P. E. 1973. The comparative anatomy of the nasal tract and the function of the spermaceti organ in the Physeteridae (Mammalia, Odontoceti). *Bijdragentot de Dierkunde*, **43**(1), 93–112.

Slater, G. J., Price, S. A., Santini, F. & Alfaro, M. E. 2010. Diversity versus disparity and the radiation of modern cetaceans. *Proceedings of the Royal Society B*, **277**, 3097–3104.

Toscano, A., Abad, M., Ruiz, F., Muñiz, F., Álvarez, G., García, E. X. M. & Caro, J. A. 2013. Nuevos restos de *Scaldicetus* (Cetacea, Odontoceti, Physeteridae) del Mioceno superior, sector occidental de la Cuenca del Guadalquivir (sur de España). *Revista Mexicana de Ciencias Geológicas*, **30**(2), 436–445.

Van Beneden, P. J. 1880. Les mysticètes à courts fanons des sables des environs d'Anvers. *Bulletin de l'Académie Royale des Sciences, des Lettres et des Beaux-Arts de Belgique, Series 2*, **50**, 11–27.

Velez-Juarbe, J., Wood, A. R., De Gracia, C. & Hendy, A. J. 2015. Evolutionary patterns among living and fossil kogiid sperm whales: evidence from the Neogene of Central America. *PLoS ONE*, **10**(4), e0123909. https://doi.org/10.1371/journal.pone.0123909

Viglino, M., Buono, M. R., Fordyce, R. E., Cuitiño, J. I. & Fitzgerald, E. M. 2018a. Anatomy and phylogeny of the large shark-toothed dolphin *Phoberodon arctirostris* Cabrera, 1926 (Cetacea: Odontoceti) from the early Miocene of Patagonia (Argentina). *Zoological Journal of the Linnean Society*, **185**(2), 511–542.

Viglino, M., Buono, M. R., Gutstein, C. S., Cozzuol, M. A. & Cuitiño, J. I. 2018b. A new dolphin from the early Miocene of Patagonia, Argentina: insights into the evolution of Platanistoidea in the Southern Hemisphere. *Acta Palaeontologica Polonica*, **63**(2), 261–277.

Werth, A. J. 2000. Feeding in marine mammals. Pp. 487–526 in K. Schwenk (ed.) *Feeding: form, function and evolution in tetrapod vertebrates*. San Diego, Academic Press.

Werth, A. J. 2004. Functional morphology of the sperm whale tongue, with reference to suction feeding. *Aquatic Mammals*, **30**, 405–418.

Werth, A. J. 2006. Mandibular and dental variation and the evolution of suction feeding in Odontoceti. *Journal of Mammalogy*, **87**, 579–588.

Associate Editor: Adrian Lister